



Published in final edited form as:

Biochemistry. 2006 November 14; 45(45): 13670–13676. doi:10.1021/bi061368x.

Thermal Stabilities of Brain Spectrin and the Constituent Repeats of Subunits

Xiuli An^{1,*}, Xihui Zhang¹, Marcela Salomao¹, Xinhua Guo¹, Yang Yang¹, Yu Wu¹, Walter Gratzer², Anthony J. Baines³, and Narla Mohandas¹

¹Red Cell Physiology Laboratory, New York Blood Center, New York, NY 10021

²King's College London, Randall Center for Molecular Mechanisms of Cell Function, Guy's Campus, London SE1 1UL, UK

³Department of Biosciences, University of Kent, Canterbury, Kent, CT2 7 NJ, UK

Abstract

The different genes that encode mammalian spectrins give rise to proteins differing in their apparent stiffness. To explore this, we have compared the thermal stabilities of the structural repeats of brain spectrin subunits (α II- and β II) with those of erythrocyte spectrin (α I- and β I). The unfolding transition mid-points (T_m) of the 36 α II- and β II-spectrin repeats extend between 24 and 82°C, with an average higher by some 10°C than that of the α I- and β I-spectrin repeats. This difference is reflected in the T_m -s of the intact brain and erythrocyte spectrins. Two of three tandem-repeat constructs from brain spectrin showed strong cooperative coupling, with elevation of the T_m of the less stable partner corresponding to coupling free energies of about -4.4 and -3.5 kcal mol⁻¹. The third tandem-repeat construct, by contrast, showed negligible cooperativity. Tandem-repeat mutants, in which a part of the 'linker' helix that connects the two domains was replaced by a corresponding helical segment from erythroid spectrin, showed only minor perturbation of the thermal melting profiles, without breakdown of cooperativity. Thus the linker regions, which tolerate few point-mutations without loss of cooperative function, have evidently evolved to permit conformational coupling in specified regions. The greater structural stability of the repeats in α II- and β II-spectrin may account, at least in part, for the higher rigidity of brain compared to erythrocyte spectrin.

Spectrin arose in evolution with the metazoa to meet the need for structures that strengthen cell adhesions and stabilize the plasma membrane against the forces of animal movement (1). The protein also plays a part in organizing plasma membrane signalling complexes (1, 2). Spectrin occurs as an ($\alpha\beta$)₂ tetramer, specialized for cross-linking actin filaments to membrane constituents. Both the α and β chains are largely made up of consecutive triple-helical repeating units of about 106 amino acids (3, 4); these act in ensemble as spacers between actin-binding domains in the β -subunits at opposite ends of the tetramers, and some contain binding sites for proteins such as ankyrin or for aminophospholipids (5, 6).

* Author for correspondence: Xiuli An, Red Cell Physiology Laboratory, 310 E 67th St, New York, NY10021, Tel: 212-570-3247; Fax: 212-570-3195. xan@nybloodcenter.org.

The number of spectrin genes increased during evolution with the advent of vertebrates. Invertebrates have one α -spectrin and, one β -spectrin with 16 complete triple-helical repeats and a β_{Heavy} subunit with 30 complete triple helices. Vertebrates have four genes encoding 'conventional' β subunits ($\beta\text{I-IV}$) that have 16 complete triple helical modules, and one β_{Heavy} subunit that has 30 triple helices ($\beta\text{V-spectrin}$) (1). Mammals have gained an additional α -spectrin by duplication of the pre-existing α -spectrin gene (7). There is now clear evidence of functional specialization of the two mammalian α -spectrins (αI and αII). The $\alpha\text{II-spectrins}$, which are closest in sequence to invertebrate α -spectrins, are abundant in the cells of complex tissues (8). They are enriched in such locations as post-synaptic contacts (9) (where complexes of signalling molecules reside) and intercalated discs (10, 11) (where forces of muscle contraction are transmitted). The importance of spectrin in the resistance of tissues to the forces generated by muscle contraction is evident in all animals: thus for example, in the worm *Caenorhabditis elegans* spectrin is required to strengthen adhesion between the body wall and the muscles beneath (12, 13). By contrast, $\alpha\text{I-spectrin}$ is abundant in enucleate red blood cells, where it imparts to the membrane the elasticity needed to survive the rigors of circulation (7, 14-15).

The functional distinction between the spectrins of mammalian tissue and erythrocyte is reflected in their physical properties. Spectrin purified from brain (comprising mainly αII and βII polypeptides, also known as fodrin) has a stiffer and straighter appearance in the electron microscope than that of the erythrocyte ($\alpha\text{I}\beta\text{I}$) spectrin (16-19), and this difference is also reflected in their hydrodynamic properties (16, 19). It might be conjectured that the "floppier" appearance of erythrocyte spectrin reflects its adaptation to the requirement for membrane elasticity.

Some 80-90% of each spectrin polypeptide is folded into the sequential triple helical modules, so it might be supposed that structural and functional differences between the proteins have a counterpart in the properties of their constituent domains. Having previously found that the repeating units of $\alpha\text{I-}$ and $\beta\text{I-spectrin}$ vary widely in their thermostabilities (20), we were prompted to examine those of $\alpha\text{II-}$ and $\beta\text{II-spectrins}$ to investigate the basis of the differences in the gross characteristics of the intact proteins. We have accordingly determined the thermal unfolding properties of each repeat of $\alpha\text{II-}$ and $\beta\text{II-spectrin}$, as well as some constructs comprising selected tandem pairs of repeats, and some with mutations in the single α -helix uniting them.

EXPERIMENTAL PROCEDURES

Materials

Pig brain was purchased from Pel-Freez Biologicals (Rogers, AR), human brain whole marathon-ready cDNA from Clontech (Mountain View, CA), Sephacryl S-500HR, pGEX-4T-2 vector and glutathione-Sepharose 4B from Amersham Biosciences (Piscataway, NJ), protease inhibitor cocktail sets II and III from Calbiochem (San Diego, CA), pET-31b(+) vector and nickel resin from Novagen (Madison, WI), QuickChange site-directed mutagenesis kit and BL21 (DE3) bacteria from Stratagene (La Jolla, CA). Restriction enzymes were from New England BioLabs (Beverly, MA), reduced-form glutathione, thrombin, IPTG, DFP and PMSF from Sigma (St. Louis, MO), SDS-PAGE and

electrophoresis reagents from Bio-Rad (Hercules, CA), and GelCode staining reagent from Pierce Biotechnology, Inc (Rockford, IL). Human erythrocyte and pig brain spectrins were purified by the methods of Tyler *et al.* (21) and Davis and Bennett (19) respectively.

Design and Subcloning of Recombinant Brain Spectrin Polypeptides

The boundaries of all repeats were defined by the SMART database (22). The design of all α II- and β II-spectrin single repeats and tandem-repeat fragments followed that for α I- and β I-spectrin fragments (20). The residue numbers of all sequences are given in Table 1. α IIR14, α IIR18, β IIR9 and β IIR11 were subcloned into the pET31b(+) vector, using NSI and XhoI. All other brain spectrin single repeats and two-repeat fragments were subcloned into the pGEX-4T-2 vector, using *Eco*RI and *Sal*I restriction enzymes upstream and downstream respectively. Three different α II-spectrin clones (23) and human brain cDNA were used to amplify the required α -II repeats. For α IIR1, α IIR2, α IIR3 and α IIR4, the template was clone JS1. For α IIR5, α IIR6, α IIR7 and α IIR8, the template was Marathon cDNA. Clone 2.7A was used as template to amplify α IIR9-10, α IIR11, α IIR12 and α IIR13. The template used to amplify the remaining α II-spectrin repeats was clone 3'DA. Similarly, three β II-spectrin clones (24) were used as templates to amplify β II-spectrin single repeats and tandem-repeat fragments. For β IIR1, β IIR2, β IIR3 and β IIR4, β IIR5, β IIR6, β IIR7 and β IIR8, the template was β 5.1, while for β IIR9 and β IIR10 it was clone β 2.1. Clone β 1.20 was the template for amplification of the remaining β II repeats. The fidelity of all the constructs was confirmed by DNA sequencing.

Generation of Linker Exchange Constructs

To define the five-amino-acid linker region, we used ClustalW (25) to align the sequences of tandem-repeat fragments α IIR12-13, α IR12-13, α I3-4, α IIR12-13, β I12-13 and β I9-10 with the sequence of PDB entry 1S35. PDB: 1S35 is the tandem-repeat β IR8-9, for which the heptad repeats and linker region have been defined (26). The replacement of α IIR12-13 linker GDSHD by the corresponding α IR12-13 linker NEAQK or α IR3-4 linker QATYW was accomplished by site-directed mutagenesis using the Stratagene QuickChange kit. The same method was used to replace β IIR12-13 linker EEAHR by β IR12-13 linker RDANE or β IR9-10 linker RDNLE. All the sequences were confirmed by DNA sequencing.

Preparation of Recombinant Polypeptides

The cDNA encoding the desired polypeptide was transformed into *E. coli* BL21. The expression, thrombin-cleavage to remove GST and purification of the polypeptides were performed as described previously (20). The products were dialyzed against phosphate-buffered isotonic saline (buffer A: 10 mM sodium phosphate, pH 7.4, 150 mM sodium chloride) and clarified before use by ultracentrifugation at 230,000g for 30 min at 4°C. Protein concentrations of the polypeptides were determined spectrophotometrically, using calculated specific absorptivities (27).

Mass Spectrometric Analysis and Sedimentation Equilibrium

Mass spectrometric analyses were performed using an Applied Biosystems (ABI, Foster City, CA) Voyager DE MALDI mass spectrometer. Spectrin polypeptide (2-10 mM) in low-

salt solution was mixed with equal volume of a 10mg/mL 3,5-dimethoxy-4-hydroxy-cinnamic acid solution (Sigma). 1 μ L of each mixture was spotted onto the MALDI plate. Spectra were calibrated against bovine serum albumin or myoglobin as external standards. Sedimentation equilibrium of all products in isotonic buffer A was performed in a Beckman Coulter ProteomeLab™ XL-A Analytical Ultracentrifuge, as described before. The rotor speed was set at 20,000 rpm and the equilibrium distributions were scanned at 280 nm. A good fit to a monodisperse ideal model was obtained in all cases.

Circular Dichroism Spectra and Thermal Unfolding

Far-UV CD spectra and temperature-induced unfolding were performed as described before (20). To determine the melting profiles, the ellipticity at 222 nm in buffer A was recorded at temperature intervals of 2°C. The data were corrected for the linear changes above and below the sigmoid melting transition, and expressed in terms of fraction unfolded. Coupling free energies, representing the conformational stabilization of one repeat in the tandem-repeat fragments by the other, were derived from van't Hoff plots of the corrected melting profiles of the isolated repeats and the lower-melting phases of those of the tandem repeats (20). Approximate free energy of unfolding of various single repeats at 37°C was also calculated as described previously (20).

RESULTS

Recombinant α II- and β II-spectrin Polypeptides

Table I lists the boundaries of the α II- and β II-spectrin repeats. The fragments, expressed as GST-fusion constructs, contained six additional amino acids from the vector at their N-termini. Mass spectrometry confirmed that all had the expected molecular mass, and sedimentation equilibrium showed them to be monodisperse and monomeric in all cases. Circular dichroism spectra were characteristic of polypeptide chains of high α -helicity.

Temperature-induced Unfolding of α II- and β II-Spectrin Single Repeats

We expressed and purified all α II- and β II-spectrin repeats and measured their thermal stabilities. All the repeats gave rise to typical sigmoidal unfolding equilibrium profiles, measured by temperature-dependence of circular dichroism at 222 nm. Figs 1A and 1C show representative corrected unfolding profiles of α II- and β II-spectrin repeats respectively. Figs 1B and 1D display the stability distribution of the repeats, in terms of the denaturation midpoints (T_m), along the α II- and β II-spectrin chains. These reveal appreciable differences from the corresponding results for erythrocyte spectrin (20). Thus, (1) whereas eight of the 36 isolated repeats of the latter are more than 50% unfolded at physiological temperature, there are only four repeats of such low stability in α II/ β II-spectrin. (2) While the T_m values of erythrocyte α I/ β I-spectrin repeats lie between 21 and 72 °C, those of α II/ β II-spectrin range from 25 to 81 °C. (3) The T_m averaged over all isolated repeats is higher by some 10 °C in α II/ β II- than in α I/ β I-spectrin (55.5, as against 46°C). The relationship between T_m and approximate free energy of unfolding of the repeats at 37°C is also shown in Figs 1B and 1D. It is approximate only because the relation between T_m and G° at the reference temperature (37°C) is not fixed inasmuch as it varies with the enthalpy of the unfolding transition.

Temperature-induced Unfolding of Tandem-Repeat Fragments

The thermal unfolding profiles of tandem-repeat fragments of erythrocyte spectrin demonstrated varying coupling, with stabilization of the less stable by the more stable unit (20); in all the cases that we examined, however, the biphasic character persisted, showing that cooperativity was by no means complete. Here we have examined the unfolding of three tandem-repeat fragments of brain spectrin, α IIR12-13, β IIR9-10 and β IIR12-13. (Two additional such fragments, β IIR10-11 and β IIR11-12, were also prepared, but problems of aggregation vitiated the quality of the data, which we did not attempt to analyze.) The fragments were chosen to embody two folding units differing most widely in stability, as seen in Fig. 1, and affording the best reflection therefore of cooperativity. As Fig 2 shows, the cooperativity is minimal in one of the fragments but large in the other two. Thus in both β IIR12-13 (Fig 2B) and α IIR12-13 (Fig 2C) the conformation of the repeat of lower stability is substantially stabilized by interaction with its more stable neighbor (T_m ca.16 and 19° respectively). The corresponding coupling free energies could be readily calculated as before (20), most usefully at the T_m of the less stable repeat in its isolated state (where its unfolding free energy is zero), and were, found to be ca. -4.4 and -3.5 kcal mol⁻¹ for α IIR12-13 and α IIR12-13 respectively. In the case of β II12-13 (Fig 3B) there is evidence (besides the large stabilization of the conformation of the less stable repeat) of a small but distinct stabilization of the more stable repeat by the attached unfolded repeat. This is not in itself remarkable, and indeed has been reported before for a similar fragment (α II16-17) of chicken brain spectrin (28).

Contribution of “Linker” Region to Cooperativity

MacDonald and Cummings (29) have inferred from secondary structure predictions by two methods that the α -helical propensities of sequences (‘linkers’) of 5 residues at the center of the α -helix uniting adjacent repeats of erythrocyte spectrin govern the conformational stability of the tandem-repeat fragment. To determine whether the properties of the two tandem repeats (α IIR12-13 and β IIR12-13) that we have found to display strong cooperativity are affected by the nature of the linker, we prepared two mutants of each. In α IIR12-13 the sequence in question was replaced by the corresponding residues of α IR12-13 and of α IR3-4; in β IIR12-13 the linker residues were replaced by the analogous residues from β IR12-13 and β IR9-10. The substituents were chosen because all the erythrocyte spectrin tandem-repeat fragments from which they derive display only weak to moderate cooperativity (20). As Fig 3A shows, the substitutions have relatively small effects on the unfolding profiles, although that of the erythroid α IR12-13 linker causes a discernible increase in stability, with no loss of cooperativity. The erythroid α IR3-4 linker engenders in addition a perceptible increase in cooperativity. Again (Fig 3B) the substitutions caused no major perturbation of the unfolding profiles of β II12-13.

MacDonald and Cummings (29) suggested that the secondary structure of the linker regions dictates the stability of folding in pairs of adjacent repeats. They also noted a partial breakdown of cooperativity when the linker region was predicted not to be helical, but this was not a large effect, because in no cases, whether the denaturing agency was heat or urea, separate melting phases were observed. MacDonald and Cummings used for predictions first the DSC routine (30), which failed to predict correctly the structure of one linker that had

been determined by crystallography, and secondly the PSIPRED routine (31), which delivered the correct answer. Since our data indicate that the relationship between cooperative coupling and linker sequence is more complex than the predictions of MacDonald and Cummings might suggest, we sought alternative means of investigating it. We made sequence alignments of highly cooperative and weakly cooperative pairs from multiple organisms, and we also ran predictions of the propensity of the sequences in the tandem pairs to form α -helices, using the program Agadir (32). Inspection of the multiple sequence alignments disclosed no motifs or characteristic arrangement of types of amino acids that distinguished the different classes of pairs (Fig 4). Likewise, Agadir gave no consistent indication of the contribution of helical propensity either in the linker or in the helices that it joins.

At present, we cannot envisage any mechanism that might allow the linker to engender cooperative folding between repeats. Batey *et al.* (28) show that mutations in the linker sequence can eliminate coupling. The only conclusion that seems compatible with all available data is that linkers between triple helical repeats have evolved to allow or exclude cooperative coupling as required.

Intact Brain Spectrin

The denaturation profile of pig brain spectrin tetramer is shown in Fig 4. This demonstrates first that there is extensive cooperative coupling between many of the repeats along the brain spectrin chains, since unfolding occurs much more sharply than calculated by merely summing the profiles of all individual repeats; secondly that the thermal stability of brain spectrin is greater than that of erythroid spectrin (T_m respectively 49.5 and 58 °C). We have assumed that the result for the brain spectrin tetramer will hold good also for the human protein, in view of the high degree of sequence conservation in mammalian species (7).

DISCUSSION

We have shown that the individual brain spectrin repeats, like those of erythroid spectrin, exhibit a wide range of thermal stabilities. The extent to which the low stability of certain of the repeats, such as α IIR12 and β IIR11, which are substantially unfolded at 37°C (Fig 1), impacts on the hydrodynamic flexibility of the intact protein remains uncertain in consequence of the extensive (though varying) stabilizing interactions between successive repeats along the chain. Thus, the tandem-repeat construct, β IIR9-10 shows little interaction between its constituent parts, whereas in β IIR12-13 the free energy of coupling at the T_m of the isolated β IIR13 is some 4.4 kcal mol⁻¹. Even here, however, the shape of the unfolding profile indicates that cooperativity is incomplete, for the perceptible shoulder in the region of the mid-point reflects a significant weight of the half-unfolded form. This contrasts with the tandem repeat α IIR16-17 of chicken spectrin, which by this criterion exhibits completely cooperative melting (28). We cannot of course, on the basis of a circular dichroism profile alone, exclude small deviations from two-state behavior, such as, for instance, comparison with a fluorescence-based profile can reveal (28).

Law *et al* (33, 34) have demonstrated that some triple helices can be unfolded in physiological conditions by an applied pulling force, well within the range of the shearing

forces encountered by the red cell in the circulation. Law *et al.* (34) have also shown that the magnitude of conformational coupling in forced unfolding diminishes with increasing temperature. As an extreme example of this, the 5-repeat fragment of erythrocyte spectrin β IR5-9 loses resistance to pulling in the atomic force microscope in two of its constituent repeats (R8-9) below 37°C (20). The resulting local extension of a repeat to 4-5 times its folded length must be supposed to occur reversibly in red cells in the circulation.

Our data reveal major evolutionary adaptations between α I- and α II-spectrins. The α I-spectrin confers on the erythrocyte membrane the elasticity required for survival in the circulation. It has 6 repeats with T_m at or below 37°C (20). These repeats show substantially incomplete conformational coupling with their neighbors. By contrast α II-spectrin has only one repeat with T_m below 37°C, and this is conformationally coupled to R13, so that the α IIIR12-13 pair has T_m substantially higher than 37°C.

It remains to consider the structural basis for the much greater stiffness of brain spectrin than erythroid spectrin, apparent from its hydrodynamic properties (16, 19) and its appearance in the electron microscope (16-19). Fig 4 shows that brain spectrin also has the greater thermal stability, as previously observed by Di Stasi *et al.* (35) for bovine brain and erythrocyte spectrins, and also high conformational coupling throughout. A high degree of stiffness could perhaps be related to the close lateral association between the α II- and β II-chains, apparent in electron microscope images of brain spectrin. Law *et al.* (36) have shown that lateral association (which in erythroid spectrin is confined to a run of four repeats in each chain at one end of the dimer (37)) promotes cooperative unfolding. Constructs of α II- and β II-spectrin, other than those containing the corresponding four repeats, show, like those of the α I- and β I-proteins (38), little interaction *in vitro* (unpublished data in this laboratory). At the same time, the greater average structural stability along the array of repeats in both brain spectrin chains, even if a few partly unfolded in the low-temperature range at the foot of the melting profile, must be expected to reduce the incidence of conformationally weak regions. The asymmetry apparent in the derivative curve in Fig. 4 suggests that there is some clustering of stable and less stable repeats in the chains, and/or of regions in which cooperativity is greater or less. The data we have presented for the entire range of repeats should assist in the selection of chain elements for further study.

Acknowledgments

This work was supported in part by NIH grants DK 26263, DK 32094 and HL31579

The abbreviations used are

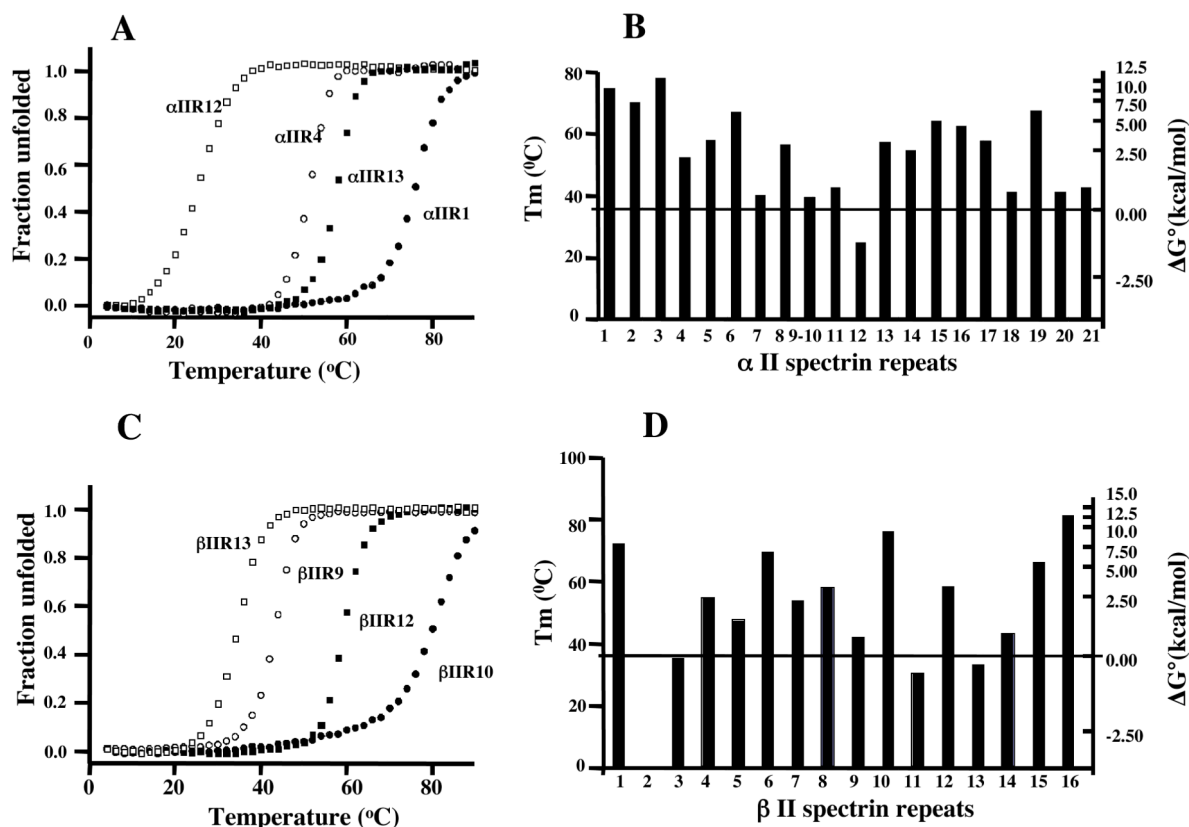
CD	circular dichroism
T_m (°C)	thermal denaturation midpoint

REFERENCES

1. Bennett V, Baines AJ. Spectrin and ankyrin-based pathways: metazoan inventions for integrating cells into tissues. *Physiol Rev.* 2001; 81:1353–92. [PubMed: 11427698]
2. Pinder JC, Baines AJ. A protein accumulator. *Nature.* 2000; 406:253–4. [PubMed: 10917516]

3. Yan Y, Winograd E, Viel A, Cronin T, Harrison SC, Branton D. Crystal structure of the repetitive segments of spectrin. *Science*. 1993; 262:2027–30. [PubMed: 8266097]
4. Speicher DW, Marchesi VT. Erythrocyte spectrin is comprised of many homologous triple helical segments. *Nature*. 1984; 311:177–80. [PubMed: 6472478]
5. Kennedy SP, Warren SL, Forget BG, Morrow JS. Ankyrin binds to the 15th repetitive unit of erythroid and nonerythroid beta-spectrin. *J Cell Biol*. 1991; 115:267–77. [PubMed: 1833409]
6. An X, Guo X, Sum H, Morrow J, Gratzer W, Mohandas N. Phosphatidylserine binding sites in erythroid spectrin: location and implications for membrane stability. *Biochemistry*. 2004; 43:310–5. [PubMed: 14717584]
7. Salomao M, An X, Guo X, Gratzer W, Mohandas N, Baines AJ. Mammalian α I-spectrin is a neofunctionalized polypeptide adapted to small, highly deformable erythrocytes. *Proc Natl Acad Sci U S A*. 2006; 103:643–8. [PubMed: 16407147]
8. Prchal JT, Papayannopoulou T, Yoon SH. Patterns of spectrin transcripts in erythroid and non-erythroid cells. *J Cell Physiol*. 1990; 144:287–94. [PubMed: 1696273]
9. Carlin RK, Bartelt DC, Siekevitz P. Identification of fodrin as a major calmodulin-binding protein in postsynaptic density preparations. *J Cell Biol*. 1983; 96:443–8. [PubMed: 6833363]
10. Bennett PM, Baines AJ, Lecomte MC, Maggs AM, Pinder JC. Not just a plasma membrane protein: in cardiac muscle cells α -II spectrin also shows a close association with myofibrils. *J Muscle Res Cell Motil*. 2004; 25:119–26. [PubMed: 15360127]
11. Baines AJ, Pinder JC. The spectrin-associated cytoskeleton in mammalian heart. *Front Biosci*. 2005; 10:3020–33. [PubMed: 15970557]
12. Moorthy S, Chen L, Bennett V. *Caenorhabditis elegans* beta-G spectrin is dispensable for establishment of epithelial polarity, but essential for muscular and neuronal function. *J Cell Biol*. 2000; 149:915–30. [PubMed: 10811831]
13. Hammarlund M, Davis WS, Jorgensen EM. Mutations in beta-spectrin disrupt axon outgrowth and sarcomere structure. *J Cell Biol*. 2000; 149:931–42. [PubMed: 10811832]
14. Knowles WJ, Morrow JS, Speicher DW, Zarkowsky HS, Mohandas N, Mentzer WC, Shohet SB, Marchesi VT. Molecular and functional changes in spectrin from patients with hereditary pyropoikilocytosis. *J Clin Invest*. 1983; 71:1867–77. [PubMed: 6863544]
15. An X, Lecomte MC, Chasis JA, Mohandas N, Gratzer W. Shear-response of the spectrin dimer-tetramer equilibrium in the red blood cell membrane. *J Biol Chem*. 2002; 277:31796–800. [PubMed: 12105217]
16. Burrige K, Kelly T, Mangeat P. Nonerythrocyte spectrins: actin-membrane attachment proteins occurring in many cell types. *J Cell Biol*. 1982; 95:478–86. [PubMed: 6183274]
17. Bennett V, Davis J, Fowler WE. Brain spectrin, a membrane-associated protein related in structure and function to erythrocyte spectrin. *Nature*. 1982; 299:126–31. [PubMed: 7110333]
18. Glenney JR Jr, Glenney P, Osborn M, Weber K. An F-actin- and calmodulin-binding protein from isolated intestinal brush borders has a morphology related to spectrin. *Cell*. 1982; 28:843–54. [PubMed: 7201352]
19. Davis J, Bennett V. Brain spectrin. Isolation of subunits and formation of hybrids with erythrocyte spectrin subunits. *J Biol Chem*. 1983; 258:7757–66. [PubMed: 6863263]
20. An X, Guo X, Zhang X, Baines AJ, Debnath G, Moyo D, Salomao M, Bhasin N, Johnson C, Discher D, Gratzer WB, Mohandas N. Conformational stabilities of the structural repeats of erythroid spectrin and their functional implications. *J Biol Chem*. 2006; 281:0527–32.
21. Tyler JM, Hargreaves WR, Branton D. Purification of two spectrin-binding proteins: biochemical and electron microscopic evidence for site-specific reassociation between spectrin and bands 2.1 and 4.1. *Proc Natl Acad Sci U S A*. 1979; 76:519296.
22. Schultz J, Milpetz F, Bork P, Ponting CP. SMART, a simple modular architecture research tool: identification of signaling domains. *Proc Natl Acad Sci U S A*. 1998; 95:5857–64. [PubMed: 9600884]
23. Moon RT, McMahon AP. Generation of diversity in nonerythroid spectrins. Multiple polypeptides are predicted by sequence analysis of cDNAs encompassing the coding region of human nonerythroid α -spectrin. *J Biol Chem*. 1990; 265:4427–33. [PubMed: 2307671]

24. Hu RJ, Watanabe M, Bennett V. Characterization of human brain cDNA encoding the general isoform of beta-spectrin. *J Biol Chem.* 1992; 267:18715–22. [PubMed: 1527002]
25. Higgins DG, Sharp PM. CLUSTAL: a package for performing multiple sequence alignment on a microcomputer. *Gene.* 1988; 73:237–44. [PubMed: 3243435]
26. Grum VL, Li D, MacDonald RI, Mondragon A. Structures of two repeats of spectrin suggest models of flexibility. *Cell.* 1999; 98:523–35. [PubMed: 10481916]
27. Perkins SJ. Protein volumes and hydration effects. The calculations of partial specific volumes, neutron scattering matchpoints and 280-nm absorption coefficients for proteins and glycoproteins from amino acid sequences. *Eur J Biochem.* 1986; 157:169–80. [PubMed: 3709531]
28. Batey S, Randles LG, Steward A, Clarke J. Cooperative folding in a multi-domain protein. *J Mol Biol.* 2005; 349:1045–59. [PubMed: 15913648]
29. MacDonald RI, Cummings JA. Stabilities of folding of clustered, two-repeat fragments of spectrin reveal a potential hinge in the human erythroid spectrin tetramer. *Proc Natl Acad Sci U S A.* 2004; 101:1502–7. [PubMed: 14747656]
30. King RD, Sternberg MJ. Identification and application of the concepts important for accurate and reliable protein secondary structure prediction. *Protein Sci.* 1996; 5:2298–310. [PubMed: 8931148]
31. Jones DT. Protein secondary structure prediction based on position-specific scoring matrices. *J Mol Biol.* 1999; 292:195–202. [PubMed: 10493868]
32. Munoz V, Serrano L. Development of the multiple sequence approximation within the AGADIR model of alpha-helix formation: comparison with Zimm-Bragg and Lifson-Roig formalisms. *Biopolymers.* 1997; 41:495–509. [PubMed: 9095674]
33. Law R, Carl P, Harper S, Dalhaimer P, Speicher DW, Discher DE. Cooperativity in forced unfolding of tandem spectrin repeats. *Biophys J.* 2003; 84:533–44. [PubMed: 12524305]
34. Law R, Liao G, Harper S, Yang G, Speicher DW, Discher DE. Pathway shifts and thermal softening in temperature-coupled forced unfolding of spectrin domains. *Biophys J.* 2003; 85:3286–93. [PubMed: 14581229]
35. Di Stasi AM, Petrucci TC, Minetti M. Comparison of thermal properties of bovine spectrin and fodrin. *Arch Biochem Biophys.* 1987; 256:144–9. [PubMed: 3038019]
36. Law R, Harper S, Speicher DW, Discher DE. Influence of lateral association on forced unfolding of antiparallel spectrin heterodimers. *J Biol Chem.* 2004; 279:16410–6. [PubMed: 14761982]
37. Ursitti JA, Kotula L, DeSilva TM, Curtis PJ, Speicher DW. Mapping the human erythrocyte beta-spectrin dimer initiation site using recombinant peptides and correlation of its phasing with the alpha-actinin dimer site. *J Biol Chem.* 1996; 271:6636–44. [PubMed: 8636080]
38. Speicher DW, Weglarz L, DeSilva TM. Properties of human red cell spectrin heterodimer (side-to-side) assembly and identification of an essential nucleation site. *J Biol Chem.* 1992; 267:14775–82. [PubMed: 1634521]

**Fig. 1.**

A. Typical thermal unfolding profiles, measured by circular dichroism at 222 nm, corrected for linear changes above and below the sigmoidal unfolding transition, of expressed single repeats of α II spectrin. The curves, from left to right, show unfolding of repeats 12, 4, 13 and 1. B. The Tm of all repeats along the α II spectrin chain. The horizontal line corresponds to physiological temperature. The scale on the right shows the approximate free energy of unfolding of the repeats at 37 $^{\circ}$ C, and applies also to the β -chain repeats in panel D. C. Typical thermal unfolding profiles for single repeats of β II spectrin, corrected as above. The curves, from left to right, are show unfolding of repeats 13, 9, 12 and 10. D. The Tm of all repeats along the β II spectrin chain.

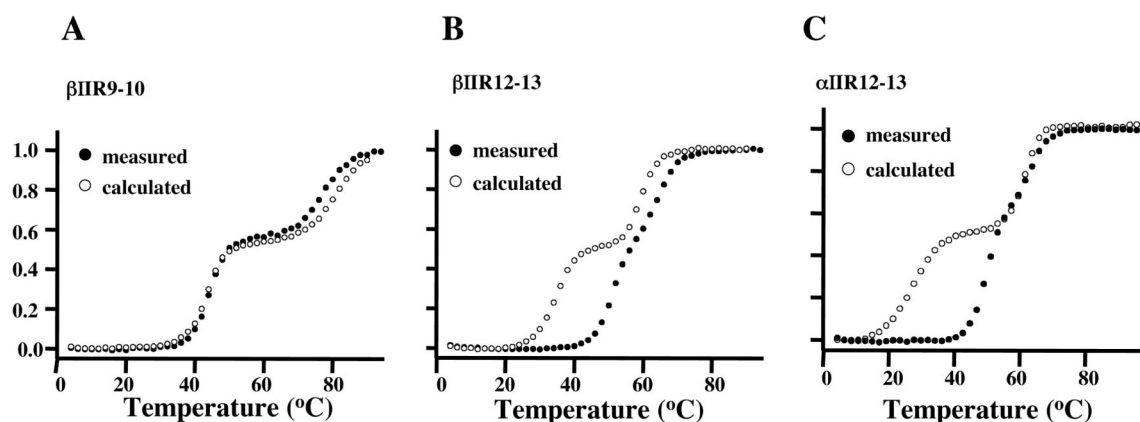
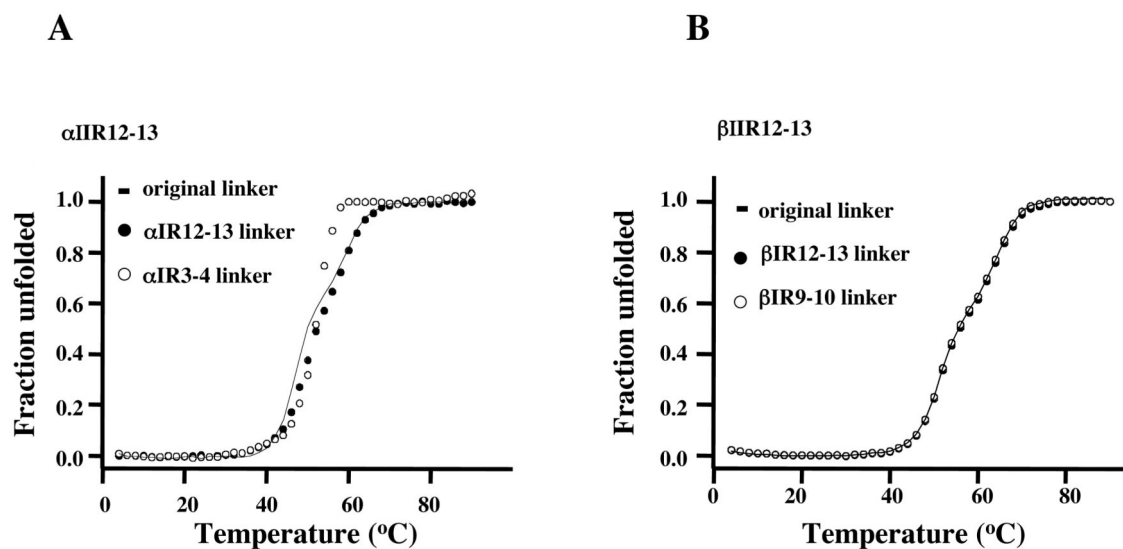


Fig. 2.

Thermal unfolding profiles of tandem repeat constructs from α II and β II spectrin chains. *A*. Fragment comprising repeats 9 and 10 of β II-spectrin; *B*. Fragment of repeats 12 and 13 of β II-spectrin; *C*. Fragment of repeats 12 and 13 of α II-spectrin. All curves are corrected for linear slopes above and below the transition. Closed circles are observed data; open circles are calculated for independent unfolding of the two repeats. Note strong cooperativity of melting of the constituent repeats in *B* and *C*, while there is no perceptible coupling of the repeats in *A*.

**Fig. 3.**

Thermal unfolding profiles of two-repeat fragments of brain spectrin with mutated linker regions. *A.* Fragment comprising repeats 12 and 13 of the α II chain: wild-type (solid line); substituent linker of α I-spectrin repeats 12 and 13 (●); substituent linker of α I-spectrin repeats 3 and 4 (○). *B.* Fragment comprising repeats 12 and 13 of the β II chain: wild-type (solid line); substituent linker of β I-spectrin repeats 12 and 13 (●); substituent linker of β I-spectrin repeats 9 and 10 (○). Note that in no case do the substitutions cause any perceptible loss of cooperativity.

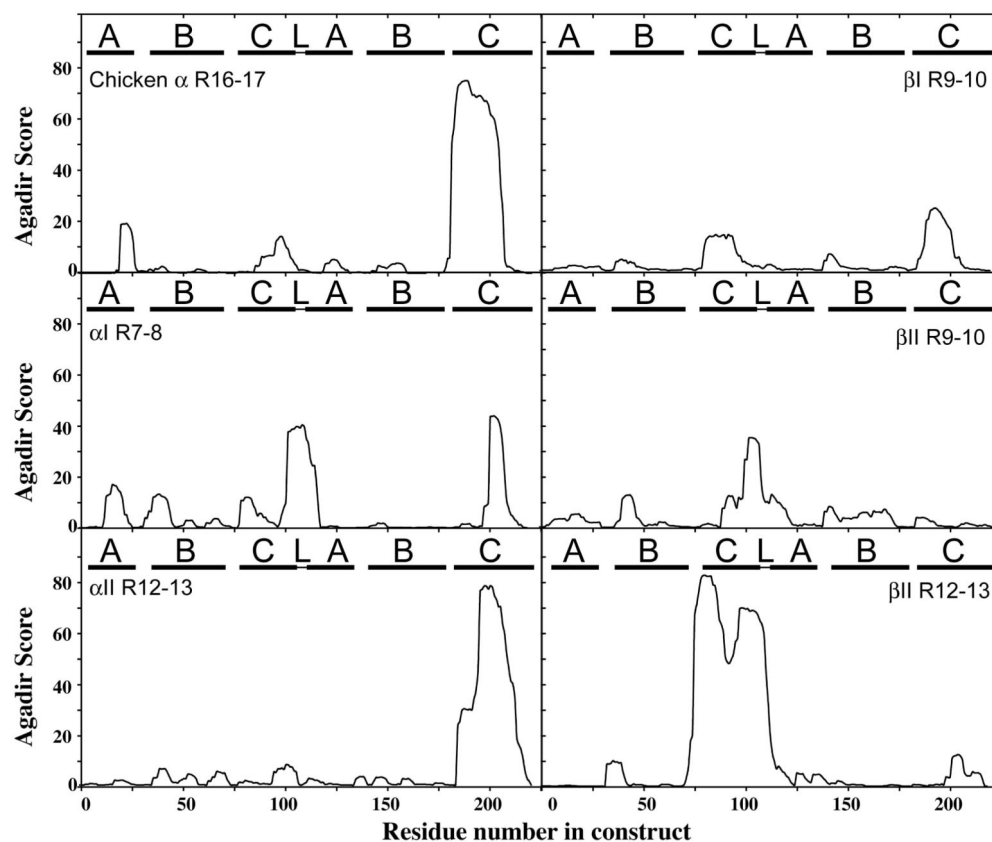


Fig. 4.

Agadir analysis of helical propensity of triple helical pairs. The figure shows predictions of helical propensity for the indicated paired spectrin repeats: chicken α -spectrin repeats 16-17 (from sequence given in PDB:1U4Q), human α I R7-8, human α II R12-13, human β I R9-10, human β II R9-10, human β II R12-13. Sequence corresponding to the helices A, B and C of the repeats is indicated as well as the linker (L) sequence.

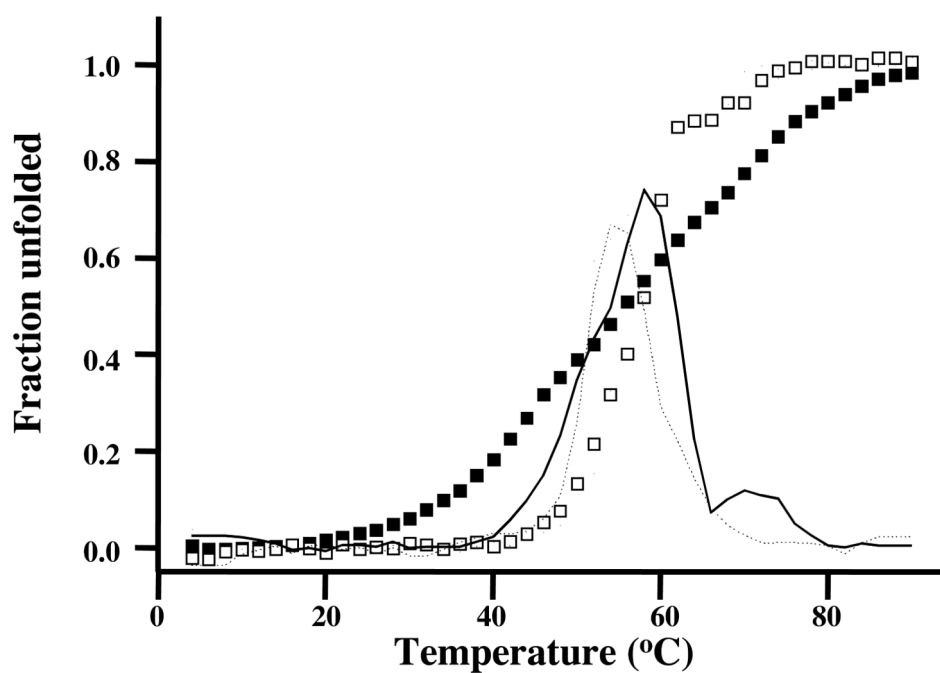


Fig. 5. Thermal unfolding profile of intact $\alpha\text{II}\beta\text{II}$ -spectrin (open squares) and the summed melting profile of all single repeats (closed squares). The first order derivative for $\alpha\text{II}\beta\text{II}$ -spectrin (solid line) and $\alpha\text{I}\beta\text{I}$ -spectrin (dashed line) are also shown.

Table 1
Information of α II and β II Spectrin Single Repeats

Name	Amino acids	Nucleotides	Name	Amino acids	Nucleotides
α IIR1	39-154	115-462	β IIR1	284 - 422	850 - 1266
α IIR2	145-260	433-780	β IIR2	418 - 533	1252 - 1599
α IIR3	251-366	751-1098	β IIR3	524 - 643	1570 - 1929
α IIR4	357-472	1069-1416	β IIR4	634 - 749	1900 - 2247
α IIR5	463-578	1387-1734	β IIR5	740 - 854	2218 - 2562
α IIR6	569-683	1705-2049	β IIR6	845 - 960	2533 - 2880
α IIR7	674-789	2020-2367	β IIR7	951 - 1067	2851 - 3201
α IIR8	780-895	2338-2685	β IIR8	1058 - 1174	3172 - 3522
α IIR9-10	886-1096	2656-3283	β IIR9	1165 - 1280	3493 - 3840
α IIR11	1087-1238	3265-3705	β IIR10	1271 - 1385	3811 - 4155
α IIR12	1229-1344	3685-4032	β IIR11	1376 - 1490	4126 - 4470
α IIR13	1335-1450	4003-4350	β IIR12	1481 - 1597	4441 - 4791
α IIR14	1441-1556	4321-4668	β IIR13	1588 - 1703	4762 - 5109
α IIR15	1547-1663	4639-4989	β IIR14	1694 - 1810	5080 - 5430
α IIR16	1654-1769	4960-5307	β IIR15	1801 - 1916	5401 - 5748
α IIR17	1760-1875	5278-5625	β IIR16	1907 - 2022	5719 - 6066
α IIR18	1866-1981	5596-5943			
α IIR19	1972-2088	5914-6264			
α IIR20	2079-2202	6235-6606			
α IIR21	2193-2317	6577-6951			

The boundaries of all repeats were defined by SMART database (<http://smart.emblheidelberg.de/>) with the exception that five amino acids are extended at both N-terminus and C-terminus to ensure proper folding. The N-terminal six amino acids are from pGEX-4T-2 vector.